Received: 14 April 2023 | Revised: 6 August 2023 | Accepted: 14 November 2023

DOI: 10.1002/jor.25729

RESEARCH ARTICLE

Journal of Orthopaedic Research®

Stem size and stem alignment affects periprosthetic fracture risk and primary stability in cementless total hip arthroplasty

Tobias Konow[1] | Katja Glismann[1] | Frank Lampe[2] | Benjamin Ondruschka[3] | Michael M. Morlock[1] | Gerd Huber[1]

[1]Institute of Biomechanics, TUHH Hamburg University of Technology, Hamburg, Germany

[2]Asklepios Klinik Barmbek, Hamburg, Germany

[3]University Medical Center Hamburg-Eppendorf, Institute of Legal Medicine, Hamburg, Germany

Correspondence
Tobias Konow, Institute of Biomechanics, TUHH Hamburg University of Technology, Denickestraße 15, Hamburg 21073, Germany.
Email: tobias.konow@tuhh.de

Funding information
DePuy Synthes

Abstract

The ideal stem size and stem position is important for the success of total hip arthroplasty, since it can affect early implant loosening and periprosthetic fractures (PPF). This study aimed to investigate how small deviations from the ideal stem size and position influences the PPF risk and primary stability. Six experienced surgeons performed preoperative templating based on which the benchmark size for each femur was determined. Consecutive implantations were performed in six cadaveric femur pairs—one side was implanted with an undersized stem followed by the benchmark size and the contralateral side with a benchmark size followed by an oversized stem (Corail, Depuy Synthes). Moreover, three different alignments (six varus, six neutral, six valgus-undersized) were compared using 18 femurs. Cortical strains during broaching and implantation were measured, and laser scans were used to determine final stem position. All specimens underwent dynamic loading. Primary stability was estimated from stem subsidence and pull-out forces. Templated stem size varied between surgeons (±1 size; $p = 0.005$). Undersizing increased stem subsidence by 320% ($p < 0.001$). Oversized stems exhibited 52% higher pull-out forces ($p = 0.001$) and 240% higher cortical strains ($p = 0.056$). Cortex strains increased with varus alignment ($R^2 = 0.356$, $p = 0.011$) while primary stability decreased with valgus stem alignment ($p = 0.043$). Surgeons should be aware that small deviations from the ideal stem size and malalignments of the stem can significantly alter the mechanical situation and affect the success of their surgery.

KEYWORDS

periprosthetic fracture, preoperative planning, primary stability, stem alignment, stem size

1 | INTRODUCTION

Loosening and periprosthetic fractures (PPF) rank within the top three reasons for revisions in cementless total hip arthroplasty (THA).[1] Risk factors for PPFs have been found to be patient-, implant-, and process-related.[2–6] Process-related factors include differences in surgical techniques and the surgeon's level of experience.[3,5] The variations in stem size chosen between surgeons[7] may either be attributed to different surgical philosophies (such as fixation in cortical or trabecular bone) or adjustments during surgery due to the surgical experience.[8,9]

Reduced primary stability and increased stem subsidence are frequently reported for undersized stems.[10–13] In contrast, the question of whether undersizing reduces or promotes PPF risk is discussed controversially in the literature.[14,15] Concerning oversized stems, the situation appears to be less controversial. Spina and Scalvi recognized that intraoperative PPF risk increases when an oversized stem is implanted[16] and Jasty and colleagues reported increasing cortical strains with increasing stem sizes.[17] However, the degree to which the selected stem size can deviate from the "ideal" size before having a significant impact on primary stability and the risk of PPF is uncertain.

The position of the implanted stem is also dependent on process-related factors such as the chosen surgical approach, the degree of exposure, and the level of surgical experience.[18] The vast majority of studies that analyzed variations in stem position examined the stem alignment in the frontal plane.[13,19–21] Lower primary stability has been associated with valgus stem alignment,[13] whereas an increased risk of PPF has been observed with varus stem alignment.[19–21]

Most studies that address stem size and position are clinical follow-up studies. Radiographic lines on X-rays have been associated with stem loosening or revisions due to PPF with an additional evaluation of the relative stem size.[11,22] The definition of over- or undersize of a stem and the extent to which it deviates from the apparent ideal stem size is not consistent.[11,13,16,23] Nonclinical studies used bone replacement models[10] and numerical approaches.[12,21,24] These approaches have limitations with regard to the accurate representation of the bone-implant interface. To address the clinical question of how the selected stem size and position affect the mechanical loading situation in the bone, it is important to investigate the impact of small deviations from the ideal stem size commonly encountered in clinical practice,[8] as well as the influence of misalignments in stem positioning using human samples.

The aim of this in vitro study was, therefore, to investigate how small deviations from the ideal stem size and variations in stem alignment influence PPF risk and the primary stability of the implant.

2 | METHODS

Cementless hip stems (Corail; Depuy Synthes) with a hydroxyapatite coating and standard offset of 135° were implanted in 15 femur pairs harvested from mostly male donors (m/f = 13/2) with an average body height of 175 ± 10 cm and age of 71 ± 17 years and stored below −20°C.[25] The Ethics Commission of the Medical Association Hamburg (WF-067/18) approved this study.

Native CT scans were acquired (Incisive CT; Philips; voxel size: $0.5 \times 0.5 \times 0.5\ mm^3$) with a calibration phantom (QSA; QRM). Hounsfield units were converted to bone mineral density (BMD) in terms of Calcium-Hydroxyapatite per milliliter (Structural Insight 3; University Medical Center Schleswig-Holstein[26]). Femur-specific BMD was determined from a $10\ mm^3$ cubic region of interest (ROI) in the head center (AVIZOLite 9.7.0; Thermo Fisher Scientific). Bone morphology was quantified (Matlab 2020b; The MathWorks) using the Cortical-Canal-Shape (CCS).[27] A higher CCS corresponds to an aged bone morphology.

2.1 | Preoperative planning

For the first part of the study, idealized two-dimensional scout views of six femoral pairs were reconstructed from CT scans and provided to six different surgeons to perform standard preoperative planning (Matlab 2020b; The MathWorks). The stem size for each femur was selected by each surgeon and the bone morphology determined based on Dorr types.[28] The median templated stem size of the six surgeons for each femur was defined as the benchmark ("ideal") stem size. The remaining nine femoral pairs were templated by the single surgeon who performed the preparation and implantation in the second part of the study. The surgeons templating philosophy was in line with the benchmark size in the first group.

2.2 | Group 1: Stem size

The six femur pairs of the first group were used to evaluate the effect of stem size. Two consecutive stem implantations were performed in each femur. In one side of a pair, first an undersized stem of one size smaller than the benchmark size was implanted and analyzed, followed by a second implantation and analysis using the benchmark stem size (Figure 1A). On the contralateral sides, the benchmark stem size was implanted first, followed by an oversized stem of one size larger (Figure 1B). Femurs were randomly assigned to the respective groups.

2.3 | Group 2: Stem alignment

The stems in the second group were implanted in three deliberate alignments into nine femur pairs (six varus benchmark size, six neutral benchmark size, six valgus undersized). Excessive lateral opening of the canal was performed to allow valgus alignment of the stems, while lateral opening was omitted for the varus alignment cases (Figure 2). No specific target angles were defined prior femur preparation. To reflect the worst-case scenario in terms of primary stability, the combination of valgus and undersized stem was chosen. The other extreme—varus in combination with an oversized stem—was not achievable.

Soft tissues were removed from all specimens before they were visually aligned using the long femoral axis and embedded into pods (Technovit 4004; Kulzer GmbH). The specimens were mounted according to the surgeon's clinical approach (anterolateral approach).

The medial region of the calcar was carefully cleaned and degreased with acetone. Three millimeters below the head resection line, approximately 20–30 round markers (Ø: 0.4 mm) were randomly placed on the medial cortex of each femur in an area of about 25 × 50 mm for the determination of cortical strains using direct image correlation (DIC).

Preparation of the femur by compaction broaches and stem implantation was performed manually (weight of the mallet: 1.4 kg) with the corresponding instruments. Dynamic impaction forces during cavity preparation were measured using a piezoelectric load cell (Kistler 9333A) placed between the broach and the broach handle (Figure 3A). Forces were recorded for the last two broaches (sample rate of

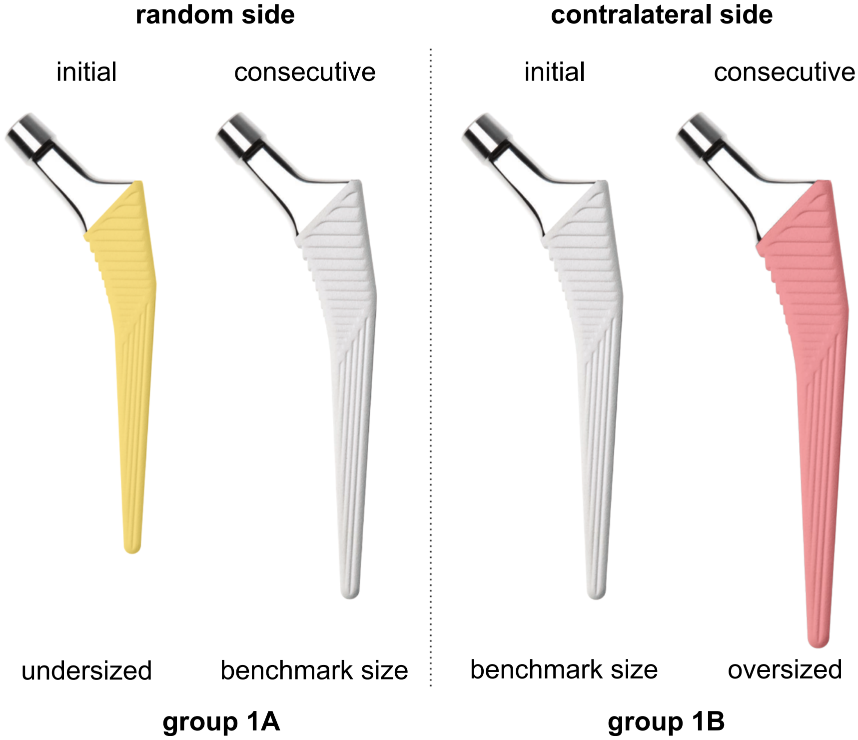

FIGURE 1 In one femur, a consecutive implantation was performed with an undersized and a benchmark stem (group 1A). The contralateral femur received a benchmark stem followed by an oversized stem (group 1B). Between the consecutive implantations, appropriate reaming was performed for the following stem.

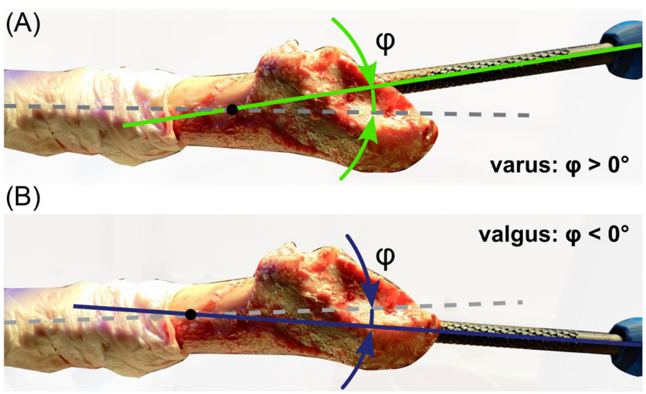

FIGURE 2 (A) Preparation of the proximal femur for a targeted varus alignment of the stem. (B) Preparation of the proximal femur for a targeted valgus alignment of the stem.

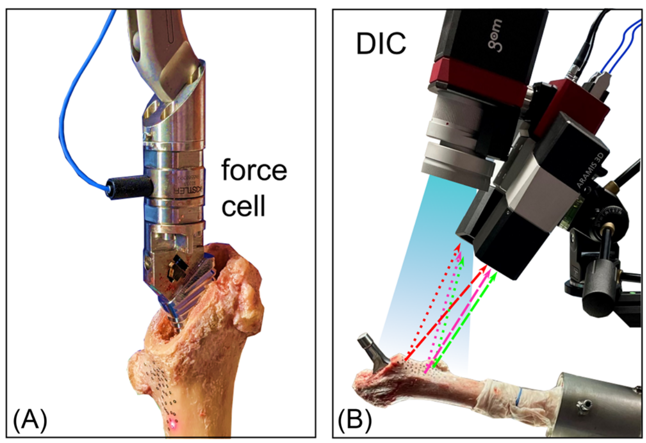

FIGURE 3 (A) The piezo load cell between the broach and the broach handle to measure forces during broaching and implantation. (B) Measurement of cortical strain using a stereo camera system and analysis based on digital image correlation.

800 kHz; LabView, National Instruments) with simultaneous continuous cortical strain measurements using digital image correlation (DIC, 25 fps, 5 µm measurement noise; ARAMIS 3D Camera; GOM) with a measurement volume of $100 \times 80 \times 50\,mm^3$ (Figure 3B).

After implantation the stem tapers were cleaned and assembled with a ceramic ball head (BIOLOX®delta; Depuy Synthes, Ø 36 mm, +5 mm). The position of the stem in the femur was acquired using laser scans (max. resolution 0.05 mm, max. accuracy 0.03 mm; HandySCAN 700, Creaform). A virtual 3D representation of the stem alignment in the femur was then reconstructed by superimposing the femoral cortices from laser scans and native qCTs (root mean square error below 0.3 mm). The canal-fill ratio (CFR) 7, vertical stem position, stem inclination, and cortical distance were evaluated using deterministic approaches to assess the size and alignment of the implanted stem relative to the femur.

2.4 | Mechanical testing

For mechanical testing the embedded specimens were aligned according to ISO 7206-4 with a 10° lateral and 9° dorsal tilt of the implant axis (2D spirit level) with respect to the loading axis and fixed in a ball and socket clamp (Figure 4A). Force-controlled cyclic loading was applied via a polyethylene covered piston to the ball head on the prosthesis using a servo-hydraulic testing machine (1 Hz; Bionix, MTS). Group 1 femora were cyclically tested using one loading condition (300 cycles; 80–800 N). Group 2 femora were loaded with two load levels (80–800 N; 80–1600 N), each applied for 600 cycles. Relative motion between the bone and the implant was measured contactless using DIC for the specimens of group 2. Recordings for 5 s were taken every 200 cycles (25 fps; measurement volume of 100 × 80 × 50 mm^3, marker size 0.4 mm, ARAMIS 3D Camera, GOM, Figure 4B). Specimens were kept moist with ringer solution. After mechanical loading, an additional laser scan was performed to determine the final stem subsidence after loading. Stems were finally removed displacement-controlled with a speed of 0.1 mm/s and pull-out forces were recorded (Z010; Zwick Roell).

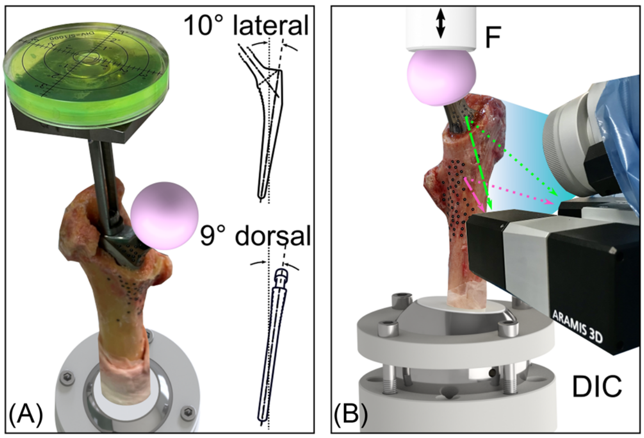

FIGURE 4 (A) 2D spirit level was used for precise alignment of the implanted stem according to ISO 7206-4 (10° lateral inclination, 9° dorsal inclination) and fixation via the ball socket holder. (B) Cyclic loading was applied to the ceramic head via a polyethylene piston. Relative motion at the bone-implant interface was measured contactless using digital image correlation.

2.5 | Statistical analysis

Statistical analysis was performed with a type I error level of 0.05 (IBM SPSS Statistics 24; IBM Corp). Unless otherwise described, the mean and standard deviation are reported. Relationships between parameters were determined using multiple Pearson correlations. Repeated-measures analyses of variance were performed to test and evaluate the eligibility of the study design with repeated implantations. Differences within a femoral pair were analyzed using paired *t* tests. Differences between conditions were examined using analyses of variance.

3 | RESULTS

BMD of trabecular bone and bone morphology were similar within femoral pairs (BMD: 359.5 ± 90.1 mgHA/cm^3, $p = 0.428$; CCS: 1.45 ± 0.26, $p = 0.695$).

3.1 | Group 1: Stem size

The preoperatively planned stem size for the six femur pairs of group 1 varied among the six surgeons by ±1 size (median stem size: 12 [size 11, size 13]; $p = 0.005$). Variations were also found in terms of the planned vertical stem position (9.7 ± 2.9 mm up to 14.6 ± 4.1 mm, $p < 0.001$).

The two consecutive stem implantations into one femur did not significantly affect the applied forces during broaching ($p = 0.685$; Figure 5A). Cortical strains, stem subsidence and pull-out forces were also similar in both groups for the benchmark stem sizes ($p = 0.746$, $p = 0.403$, $p = 0.077$; Figure 5B,C) allowing pooling of the data for further analysis.

Cortical strains were similar during broaching and stem implantation (broaching: 580 ± 1090 με, implantation: 580 ± 810 με, $p = 0.979$). Higher cortical strains were observed with larger relative stem sizes (CFR; $R^2 = 0.267$, $p = 0.010$). The highest cortical strains on the medial side were measured for oversized stems ($p = 0.056$, local peak strains up to 5.200 με; Figure 6A).

Undersized stems showed more stem subsidence than benchmark stems or oversized stems ($p = 0.001$; Figure 6B). The femoral morphology

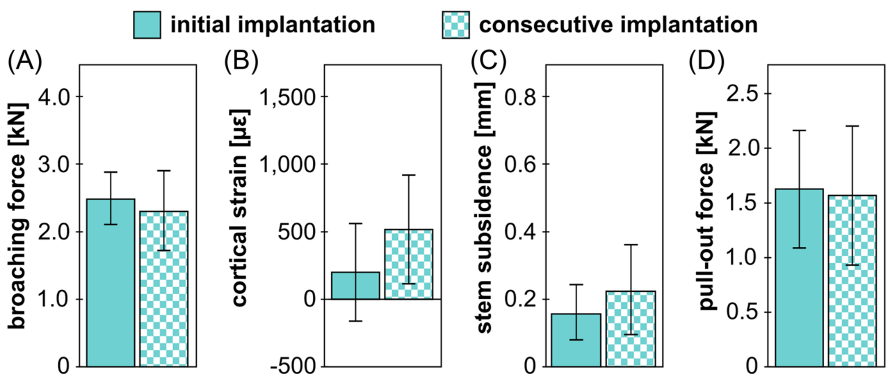

FIGURE 5 Broaching forces (A), cortical strain (B), stem subsidence (C), and pull-out forces (D) for initial and consecutive stem implantations (shown are means and standard deviations).

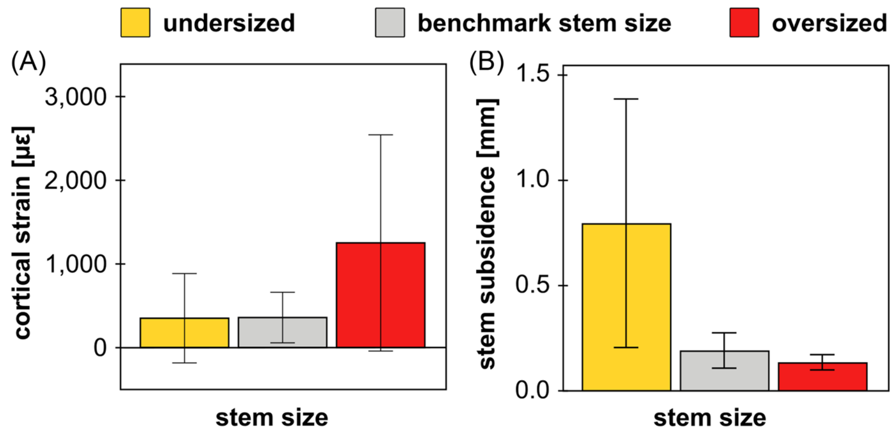

FIGURE 6 (A) Cortical strain measured at the proximal medial cortex for the three stem size groups. (B) Stem subsidence during mechanical loading with respect to the stem size groups (shown are mean and standard deviation).

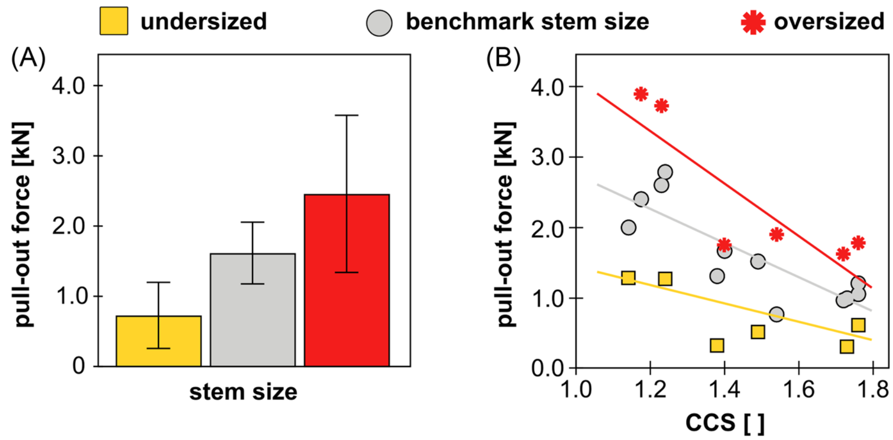

FIGURE 7 (A) Pull-out force in relation to the implanted stem size (mean and standard deviation). (B) Pullout forces decrease with increasing CCS for the three different stem size groups.

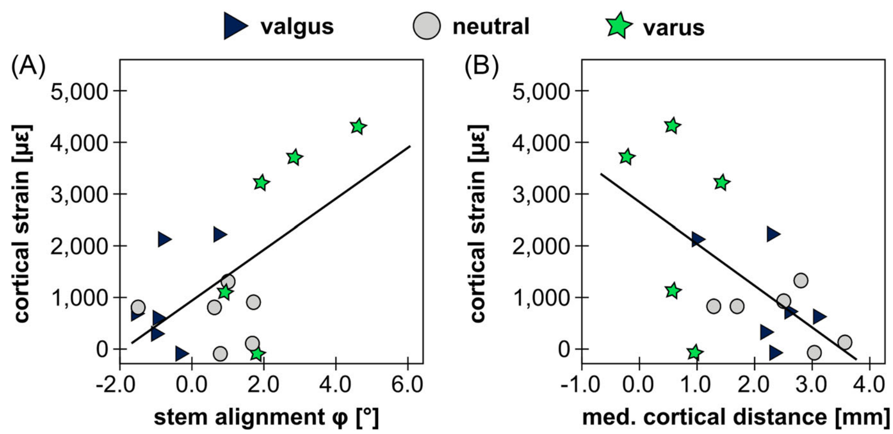

FIGURE 8 (A) Influence of stem alignment on the cortical strains on the medial proximal cortex showing an increase with a change from valgus to varus. (B) Influence of the medial cortical distance on the cortical strains on the medial proximal cortex showing a decrease in strain with a change from varus to neutral and valgus.

had no effect on the stem subsidence. Oversized stems showed higher pull-out forces compared to benchmark stems ($p = 0.008$), while implantation of undersized stems resulted in lower pull-out forces ($p = 0.007$; Figure 7A). Concurrently, femoral morphology influenced pull-out forces for all stem sizes showing a decrease in force with increasing CCS (oversized: $R^2 = 0.740$, $p = 0.028$; benchmark: $R^2 = 0.700$, $p = 0.001$; undersized: $R^2 = 0.546$, $p = 0.093$, $1 - \beta = 0.3745$; Figure 7B).

3.2 | Group 2: Stem alignment

The achieved alignment of the stem matched the intended alignment of the stem in most cases but the angular difference in the AP plane between the valgus and the neutral alignment was only 1° ($\varphi_{valgus} = -0.65 \pm 0.78°$, $\varphi_{neutral} = 0.72 \pm 1.17°$, $\varphi_{varus} = 2.42 \pm 1.41°$, $p = 0.002$; Figure 8A). A varus stem alignment resulted in a reduced distance to the medial cortex ($D_{Kort,varus} = 0.67 \pm 0.60$ mm, $D_{Kort,neutral} = 2.48 \pm 0.85$ mm, $p = 0.003$; Figure 8B). Varus stem alignment caused an increase in cortical strains ($R^2 = 0.356$, $p = 0.011$; Figure 8A) similar as the reduced cortical distance ($R^2 = 0.387$, $p = 0.008$; Figure 8B). In contrast, a valgus stem alignment did neither affect the distance to the medial cortex ($D_{Kort,valgus} = 2.26 \pm 0.70$ mm, $p > 0.999$; Figure 8B) nor the cortical strains ($p = 0.500$).

The primary stability of stems in varus was increased as stem subsidence tended to be lower (varus: 0.041 ± 0.026 mm, neutral/valgus: 0.351 ± 0.765 mm, $p = 0.100$) and measured pull-out forces were higher (varus: 2521 ± 1382 N, neutral: 2147 ± 1250 N, $p = 0.043$). However, higher translational relative motions were observed for stems with a varus alignment (varus: 17 ± 11 µm, neutral/valgus: 8 ± 2 µm, $p = 0.043$). Lastly, increased stem subsidence was found for undersized stems with a valgus alignment (valgus: 0.423 ± 0.740 mm, neutral/varus: 0.232 ± 0.432 mm, $p = 0.043$) and lower pull-out forces were measured compared to benchmark-sized stems with neutral or varus stem tilt (valgus: 1527 ± 1038 N, $p = 0.043$).

4 | DISCUSSION

The six experienced surgeons exhibited a variation of ±1 stem size during templating. In in vitro experiments, this small variation lead to stem subsidence in case of undersized stems and to higher cortical strains for oversized stems or varus alignment.

The femur pairs used for stem implantations showed little variations with respect to bone quality and bone morphology and no outliers with for example, like osteoporotic bone, which is more common in elderly females.[6] The specimens such represent a standard patient collective receiving uncemented primary THA.

4.1 | Methodology and limitation

Defining the benchmark size on the planning of several surgeons is regarded as more representative for the clinical situation than a size based on the choice of a single surgeon.[11,12,17,24]

Studies using paired femurs reduce the effects of patient-specific factors for the comparison between two levels of an independent factor. In this study, a new approach was introduced to even further reduce the influence of patient specific factors by performing consecutive implantations in the same femur. This approach additionally has the economic effect that fewer human specimens are needed. It could be shown that this proceeding does not affect the interface between stem and bone if broaching for one size larger is performed. This supports the existing clinical practice of implanting the next stem size when intraoperative primary stability is not achieved with the selected stem size. Previous studies using consecutive implantations have been performed without validation.[17,29]

Due to limited availability, cadaveric studies have to deal with small sample sized and low power of the experiment. Further it is limited to the single type of implant which is a fully porous HA-coated tapered wedge stem (Corail) and provides metaphyseal and diaphyseal contact. Undersized valgus stems were compared to bench-mark sized implants in different stem orientations but not to varus oversized, since the surgeon was not able to implant them.

4.2 | PPF risk

The choice of stem size influences the periprosthetic fracture risk. Higher medial cortical stresses with implantations of oversized stems have already been reported [16,17] and even slightly oversized stems (by one size) result in a larger amount of removed bone. Additionally, larger preparation broaches are related to higher preparation forces and cortical strains.[30] The magnitude of the local strain peaks of 5200 µε measured during the implantation of oversized stems are close to the critical fracture range of 5500–10000 µε.[17,31] In contrast to Bonnin and colleagues who indicated an increased risk of PPF when oversized stems were implanted in small a.p. diameter femora,[32] no increase in cortical strains associated with a Dorr Type A femoral morphology (small CCS) was observed in this study. Implantation of an oversized stem into a Dorr Type C femur with an aged bone morphology could increase the risk of PPF due to the higher broaching and impaction forces combined with a reduced distance to thin, fragile cortical bone, as cautioned already in the literature.[15]

Stem alignment is shown to affect strain and such the PPF risk. The highest cortical strains were observed when stems were implanted in varus which is consistent with other studies.[19–21] The observed mean cortical strains between 3200 and 4300 µε were associated with local strain peaks of 8000 µε, which lie within the critical range for fracture initiation between 5500 and 10,000 µε.[17,31] The reduced distance between the stem and the cortex due to varus stem alignment inevitably leads to a decreased thickness of the trabecular layer between stem and cortex. This reduces the force-distributing and dampening effect of the trabecular layer and might promote an uneven load distribution with higher local loads on the cortex.[20] In addition to the altered loading situation of the bone, incorrect stem alignment also affects the reconstruction of the head center of rotation.[18]

4.3 | Primary stability

The relationship between the primary stability of the stem and bone quality or morphology has been established in previous studies,[33,34] the present findings particularly emphasize the influence of stem size on primary stability. The higher primary stability of oversized stems can be attributed to the higher degree of canal filling ratio in the proximal femur and tighter fit of the stem. Vice versa the highest stem subsidence (~0.8 mm) was found for undersized stems when loaded with single body weight (800 N). Higher loads may further increase stem subsidence and might cause critical subsidence during the initial phase after implantation preventing ingrowth (1.2–3 mm[35,36]) or the initiation of a PPF due to excessive stem subsidence.[14] The lower pullout forces for undersized stems are in line with observations from previous studies and further underline the importance to avoid undersizing.[13,23,33,35] Primary stability as assessed in this study was improved for stems with a varus malalignment, but the higher relative motions between bone and stem also observed may negatively influence bone ingrowth. The lower primary stability observed for valgus undersized stems cannot be clearly attributed to the valgus alignment, as it could just as well have been caused by the smaller stem size.

5 | CONCLUSION

Surgeons should be aware that for fully porous HA-Coated tapered wedge stems such as the Corail even minor deviations from the ideal stem size, can significantly alter the mechanical situation and may affect primary stability or PPF risk and such the success of the own surgery. Malalignment of the stem, especially into varus direction, was shown to significantly increase cortical loading and thus the PPF risk in addition to altering the physiologic reconstruction of the joint center.

AUTHOR CONTRIBUTIONS

Tobias Konow: Study design; methodology; testing; investigation; formal analysis; writing—original draft. **Katja Glismann**: Methodology; writing—original draft. **Frank Lampe**: Implantations. **Benjamin Ondruschka**: Specimen selection; harvesting & imaging. **Michael M. Morlock**: Statistical analysis; writing—review & editing. **Gerd Huber**: Study design; project coordination; writing—review & editing. All authors have read and approved the submitted manuscript.

ACKNOWLEDGMENTS

The authors would like to thank Depuy Synthes for providing the prosthesis components, surgical tools, and financial support. Open Access funding enabled and organized by Projekt DEAL.

CONFLICTS OF INTEREST STATEMENT

F. L. is a paid consultant of Depuy Synthes and Aesculap. B. O. is a board member of the German Society of Legal Medicine. M. M. M. is a paid consultant of DePuy Synthes and obtains research support as a Principal Investigator from Ceramtec, DePuy and Beiersdorf. He obtains speaker's fees from Aesculap, Ceramtec, DePuy, Zimmer, Peter Brehm, Corin and Mathys and is in the editorial board "Trauma und Berufskrankheit." G. H. is an associated member of the board of the German Society of Biomechanics.

ORCID

Tobias Konow http://orcid.org/0000-0002-5265-997X

REFERENCES

1. Grimberg A, Lützner J, Melsheimer O, et al. *Jahresbericht 2022*. EPRD Deutsche Endoprothesenregister; 2022.
2. Haddad FS. Periprosthetic fractures: more challenges ahead. *Bone Joint J*. 2020;102-B(5):547-549.
3. Konow T, Baetz J, Melsheimer O, Grimberg A, Morlock M. Factors influencing periprosthetic femoral fracture risk. *Bone Joint J*. 2021;103-B(4):650-658.
4. Lamb JN, Baetz J, Messer-Hannemann P, et al. A calcar collar is protective against early periprosthetic femoral fracture around cementless femoral components in primary total hip arthroplasty. *Bone Joint J*. 2019;101-B(7):779-786.
5. Australian Orthopaedic Association National Joint Replacement Registry. *Hip, Knee & Shoulder Arthroplasty: Annual Report 2017*. AOANJRR; 2017:1-380.
6. Berend ME, Smith A, Meding JB, Ritter MA, Lynch T, Davis K. Long-term outcome and risk factors of proximal femoral fracture in uncemented and cemented total hip arthroplasty in 2551 hips. *J Arthroplasty*. 2006;21(6 suppl):53-59.
7. Konow T, Bätz J, Beverland D, et al. Variability in femoral preparation and implantation between surgeons using manual and powered impaction in total hip arthroplasty. *Arthroplast Today*. 2022;14:14-21.
8. Holzer LA, Scholler G, Wagner S, Friesenbichler J, Maurer-Ertl W, Leithner A. The accuracy of digital templating in uncemented total hip arthroplasty. *Arch Orthop Trauma Surg*. 2019;139(2):263-268. doi:10.1007/s00402-018-3080-0
9. The B, Verdonschot N, van Horn JR, van Ooijen PMA, Diercks RL. Digital versus analogue preoperative planning of total hip arthroplasties. *J Arthroplasty*. 2007;22(6):866-870.
10. Fottner A, Woiczinski M, Kistler M, et al. Influence of undersized cementless hip stems on primary stability and strain distribution. *Arch Orthop Trauma Surg*. 2017;137(10):1435-1441.
11. Magill P, Hill J, O'Brien S, Stevenson M, Machenaud A, Beverland D. Observed effect of femoral component undersizing and a collarless design in the development of radiolucent lines in cementless total hip arthroplasty. *Arthroplast Today*. 2020;6(1):99-103.
12. Cristofolini L, Erani P, Bialoblocka-Juszczyk E, et al. Effect of undersizing on the long-term stability of the Exeter hip stem: a comparative in vitro study. *Clin Biomech*. 2010;25(9):899-908.
13. Kutzner KP, Freitag T, Donner S, Kovacevic MP, Bieger R. Outcome of extensive varus and valgus stem alignment in short-stem THA: clinical and radiological analysis using EBRA-FCA. *Arch Orthop Trauma Surg*. 2017;137(3):431-439.
14. Korsnes L, Gottvall A, Buttazzoni C, Mints M. Undersizing the Exeter stem in hip hemiarthroplasty increases the risk of periprosthetic fracture. *HIP Int*. 2020;30(4):469-473. http://journals.sagepub.com/doi/10.1177/1120700019855313
15. Li M, Zeng Y, Wu Y, Liu Y, Wu L, Shen B. Cementless femoral stems with lower canal fill ratio have similar mid-term to long-term

outcomes to those with adequate fill ratio in Dorr type C femurs. *Arch Orthop Trauma Surg*. 2022;142(6):1265-1273. doi:10.1007/s00402-021-03916-x
16. Spina M, Scalvi A. Periprosthetic fractures of the proximal femur within first year of the index hip prosthesis. *Acta Biomed Ateneo Parmense*. 2020;91(3):2020060.
17. Jasty M, Henshaw RM, O'Connor DO, Harris DH. High assembly strains and femoral fractures produced during insertion of uncemented femoral components. *J Arthroplasty*. 1993;8(5):479-487.
18. Haversath M, Lichetzki M, Serong S, et al. The direct anterior approach provokes varus stem alignment when using a collarless straight tapered stem. *Arch Orthop Trauma Surg*. 2021;141(6):891-897. doi:10.1007/s00402-020-03457-9
19. Sidler-Maier CC, Waddell JP. Incidence and predisposing factors of periprosthetic proximal femoral fractures: a literature review. *Int Orthop*. 2015;39(9):1673-1682.
20. Tadross TSF, Nanu AM, Buchanan MJ, Checketts RG. Dall-Miles plating for periprosthetic B1 fractures of the femur. *J Arthroplasty*. 2000;15(1):47-51.
21. Kwak DK, Bang SH, Lee SJ, Park JH, Yoo JH. Effect of stem position and length on bone-stem constructs after cementless hip arthroplasty. *Bone Joint Res*. 2021;10(4):250-258.
22. Buttaro MA, Oñativia JI, Slullitel PA, et al. Metaphyseal debonding of the Corail collarless cementless stem: report of 18 cases and case-control study. *Bone Joint J*. 2017;99B(11):1435-1441.
23. D'Ambrosio A, Peduzzi L, Roche O, Bothorel H, Saffarini M, Bonnomet F. Influence of femoral morphology and canal fill ratio on early radiological and clinical outcomes of uncemented total hip arthroplasty using a fully coated stem. *Bone Joint Res*. 2020;9(4):182-191.
24. Al-Dlrini RMA, O'Rourke D, Huff D, Martelli S, Taylor M. Biomechanical robustness of a contemporary cementless stem to surgical variation in stem size and position. *J Biomech Eng*. 2018;140(9):1-12.
25. Püschel K, Heinemann A, Dietz E, Hellwinkel O, Henners D, Fitzek A. New developments and possibilities in the field of post-mortem medicine mortui vivos docent. *Rechtsmedizin*. 2020;30(6):425-429.
26. Graeff C, Timm W, Nickelsen TN, et al. Monitoring teriparatide-associated changes in vertebral microstructure by high-resolution CT in vivo: results from the EUROFORS study. *J Bone Miner Res*. 2007;22(9):1426-1433.
27. Konow T, Schlieker PJ, Lampe F, et al. Influence of bone morphology and femur preparation method on the primary stability of hip revision stems. *J Orthop Res*. 2023;41(6):1283-1290.
28. Dorr LD, Faugere M-C, Mackel AM, Gruen TA, Bognar B, Malluche HH. Structural and cellular assessment of bone quality of proximal femur. *Bone*. 1993;14(3):231-242.
29. Elias JJ, Nagao M, Chu Y-H, Carbone JJ, Lennox DW, Chao EYS. Medial cortex strain distribution during noncemented total hip arthroplasty. *Clin Orthop Relat Res*. 2000;370(370):250-258.
30. Oberst S, Baetz J, Campbell G, et al. Vibro-acoustic and nonlinear analysis of cadavric femoral bone impaction in cavity preparations. *MATEC Web Conf*. 2018;148:14007.
31. Bayraktar HH, Morgan EF, Niebur GL, Morris GE, Wong EK, Keaveny TM. Comparison of the elastic and yield properties of human femoral trabecular and cortical bone tissue. *J Biomech*. 2004;37(1):27-35.
32. Bonnin MP, Neto CC, Aitsiselmi T, Murphy CG, Bossard N, Roche S. Increased incidence of femoral fractures in small femurs and women undergoing uncemented total hip arthroplasty—why? *Bone Joint J*. 2015;97-B(6):741-748.
33. Rattanaprichavej P, Laoruengthana A, Chotanaphuti T, Khuangsirikul S, Phreethanutt C, Pongpirul K. Subsidence of hydroxyapatite-coated femoral stem in Dorr type C proximal femoral morphology. *J Arthroplasty*. 2019;34(9):2011-2015.
34. Nazari-Farsani S, Vuopio ME, Aro HT. Bone mineral density and cortical-bone thickness of the distal radius predict femoral stem subsidence in postmenopausal women. *J Arthroplasty*. 2020;35(7):1877-1884. doi:10.1016/j.arth.2020.02.062
35. Streit MR, Haeussler D, Bruckner T, et al. Early migration predicts aseptic loosening of cementless femoral stems: a long-term study. *Clin Orthop Relat Res*. 2016;474(7):1697-1706.
36. Karrholm J, Borssen B, Lowenhielm G, Snorrason F. Does early micromotion of femoral stem prostheses matter? 4-7-year stereoradiographic follow-up of 84 cemented prostheses. *J Bone Joint Surg Br*. 1994;76-B(6):912-917.

How to cite this article: Konow T, Glismann K, Lampe F, Ondruschka B, Morlock MM, Huber G. Stem size and stem alignment affects periprosthetic fracture risk and primary stability in cementless total hip arthroplasty. *J Orthop Res*. 2023;1-8. doi:10.1002/jor.25729